Supporting Information

The Carrier Dynamics for Self-assembled Black Phosphorus and Perovskite Nanocrystal Enable Photocatalytic Conversion

Jing Ji, [a] Hang Yin, *[a] Xin Zhou, [a] Bingxi Song, [a] Xuhui Feng, [b] Peiqing Cai, [b] Laishun Qin, *[a] Yuexiang Huang, [a] Jianyong Liu, [c] Da Chen*[a]

[a] Jing Ji, Hang Yin, Xin Zhou, Bingxi Song, Laishun Qin, Yuexiang Huang, Da Chen
College of Materials and Chemistry, China Jiliang University, Hangzhou 310018, China
E-mail: yinhang@cjlu.edu.cn E-mail: dchen_80@hotmail.com
[b] Xuhui Feng, Peiqing Cai
College of Optical and Electronic Technology, China Jiliang University, Hangzhou 310018, China
[c] Jianyong Liu
State Key Laboratory of Molecular Reaction Dynamics, Dalian Institute of Chemical Physics, Chinese Academy of Science, Dalian 116023, China

Corresponding Author
*yinhang@cjlu.edu.cn
*qinlaishun@cjlu.edu.cn
*dchen_80@hotmail.com

Contents

Theoretical Methods.....S1
Figure S1.....S2
Figure S2.....S2
Figure S3.....S2
Figure S4.....S3
Figure S5.....S3
Figure S6.....S3
Figure S7.....S4
Figure S8.....S4
Figure S9.....S4
Figure S10.....S5
Figure S11.....S5
Figure S12.....S6
Figure S13.....S6
Figure S14.....S6
Figure S15.....S7
Figure S16.....S7
Figure S17.....S8
Figure S18.....S8
Figure S19.....S8
Table S1.....S9
Table S2.....S9

S1. Theoretical Methods

Theoretical Calculation of Weak Interaction: The weak interaction for the intermediates were calculated by sign(λ_2)ρ function, and plotted by independent gradient model (IGM). The IGM is an effective method to estimate the the non-covalent interactions in hybrid materials. As similar to RDG method, the weak inter- and intra-molecular interactions were calculated by the function of sign(λ_2)ρ and the δ_g index.

Here, we summarize the IGM method considering two given fragments, i.e. $CsPbBr_3$ and BP framework. Given a geometry, the electron density (ED) ρ is computed at each node of a grid encompassing the molecular system. Its gradient $\nabla\rho$ is also computed. Afterwards, the fragment components of the true ED gradient ($\frac{\partial\rho_A}{\partial x}, \frac{\partial\rho_B}{\partial x}$) are determined by equation S1 (using the gradient based partition (GBP) when the ED is derived from a wave function).

$$\frac{\partial\rho}{\partial x} = \left|\frac{\partial\rho_A}{\partial x} + \frac{\partial\rho_B}{\partial x}\right| \qquad \text{S1}$$

Between $CsPbBr_3$ and BP framework, the two individual gradient contributions have opposite signs, which mean that the fragment EDs mix when the two fragments approach each other. This overlap between ED clouds results in an attenuation of the total ED gradient in the region between fragments. To quantify this attenuation, we simultaneously consider two molecular models: the interacting (real) system, and a non-interacting reference (i.e., the so-called independent gradient model (IGM)). At a given point of the grid, for the real system featuring the interaction, the true ED gradient is:

$$\frac{\partial\rho_{IGM}}{\partial x} = \left|\frac{\partial\rho_A}{\partial x} + \frac{\partial\rho_B}{\partial x}\right| \qquad \text{S2}$$

The norm $\left|\nabla\rho_{IGM}\right|$ resulting from equation S2 represents an upper limit of the norm $\left|\nabla\rho\right|$ of the true ED gradient. Thereby, we calculate the local δ_g descriptor as follows:

$$\delta_g = \left|\nabla\rho_{IGM}\right| - \left|\nabla\rho\right| \qquad \text{S3}$$

which quantifies the contragradience between the two fragment ED sources. Non-zero values of δ_g exclusively correspond to interaction situations: the larger δ_g, the stronger the interaction.

S2. Figures

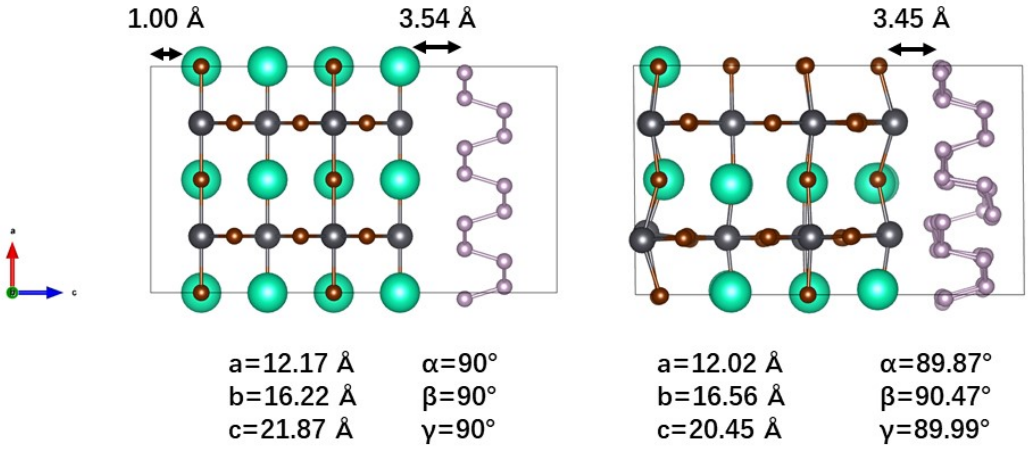

Figure S1. The reconstructed interfacial model with initial lattice parameters and optimized lattice parameters, respectively.

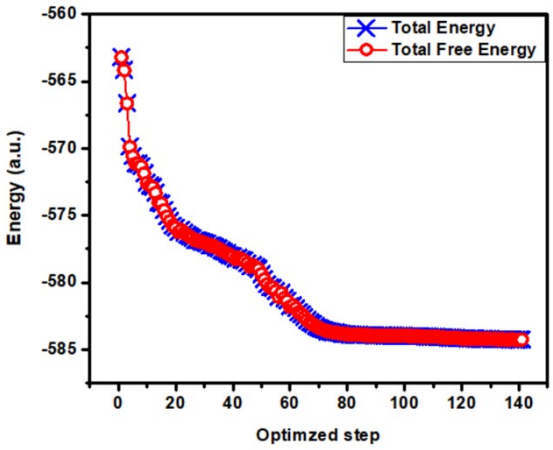

Figure S2. The optimized total energy and free energy corresponding to each step for reconstructed interfacial model.

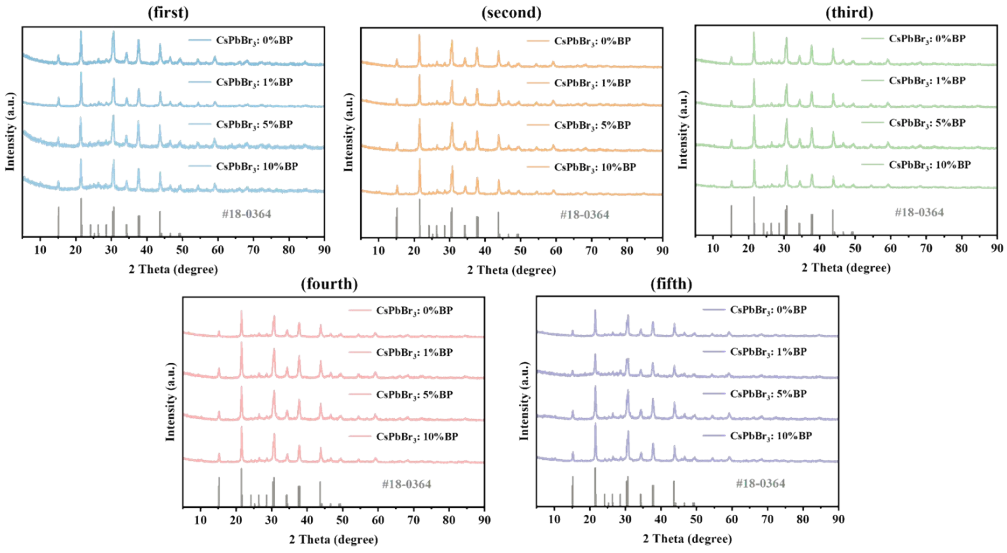

Figure S3. XRD patterns of $CsPbBr_3$: x%BP (x = 1, 5, 10) NCs for five synthesis procedures.

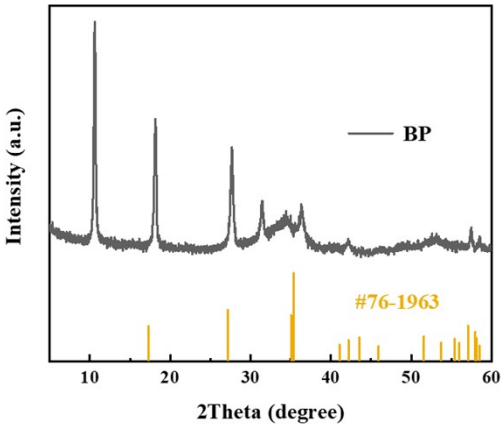

Figure S4. XRD patterns of pure BP and standard JCPDS data (No.76-1963).

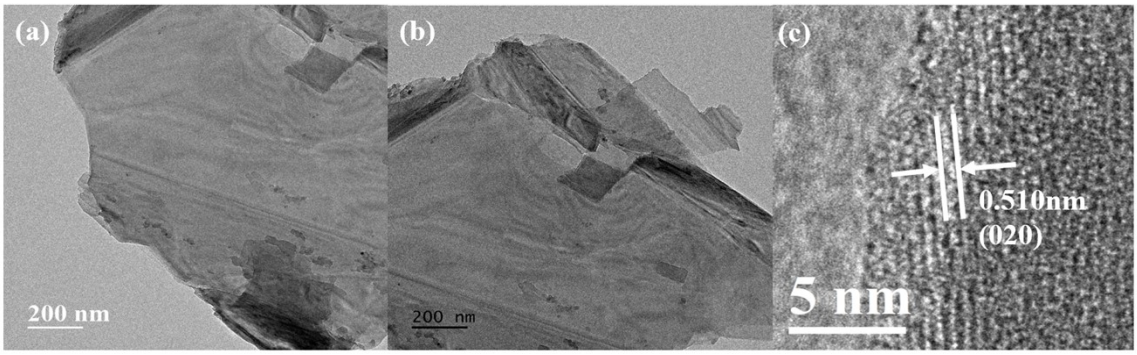

Figure S5. (a-b) TEM images and (c) HRTEM images of pure BP.

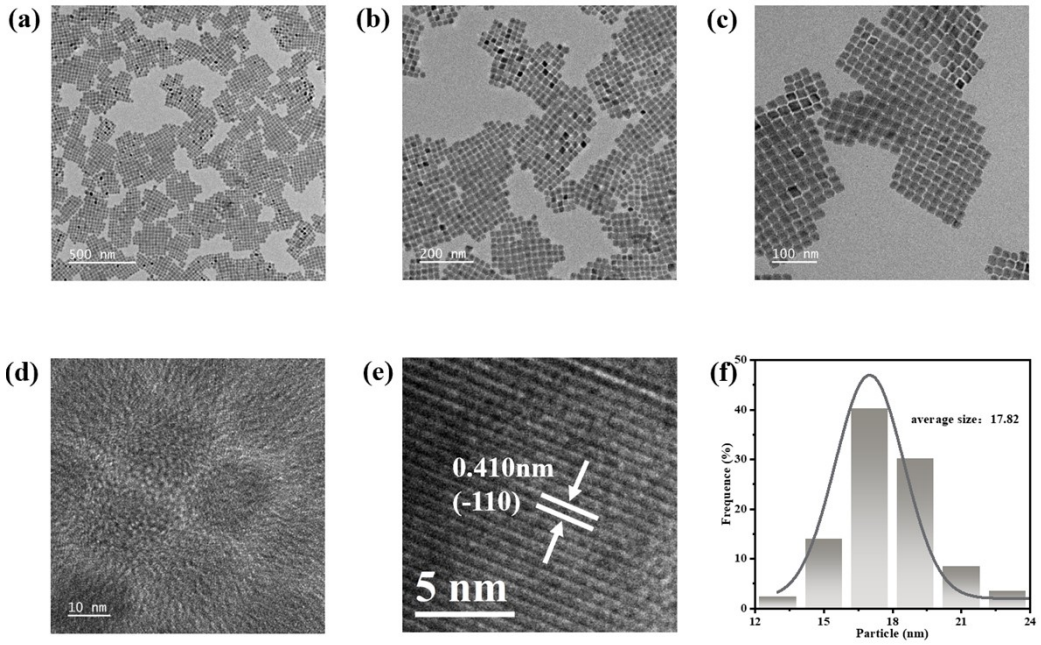

Figure S6. (a-d) TEM images, (e) HRTEM and (f) the size distribution images of $CsPbBr_3$ NCs.

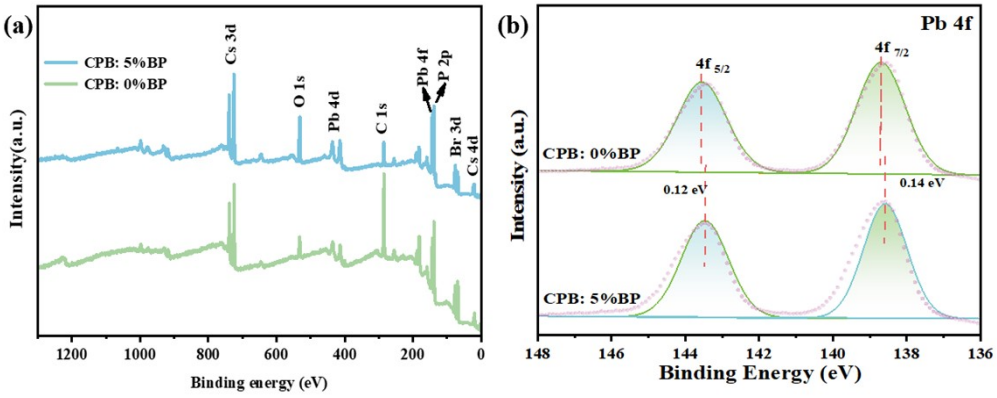

Figure S7. (a) XPS full-scan spectra of the $CsPbBr_3$ and BP. (b) XPS valence band spectra of the $CsPbBr_3$ and BP.

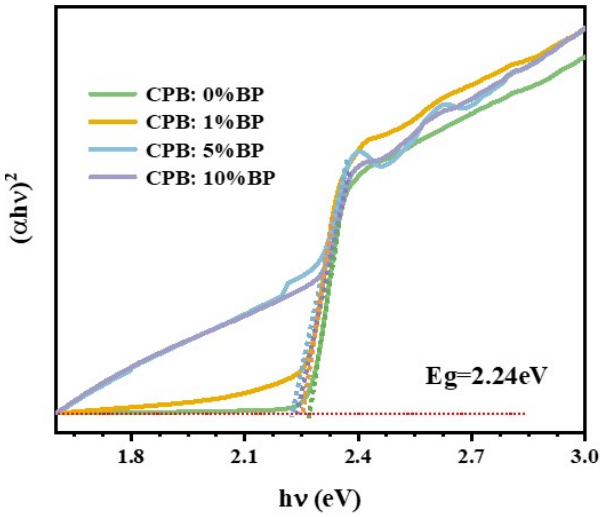

Figure S8. The band gap values of $CsPbBr_3$: x%BP (x%= 0%, 1%, 5%, 10%) estimated from the plotted curves of $(\alpha h\nu)^2$ vs hν.

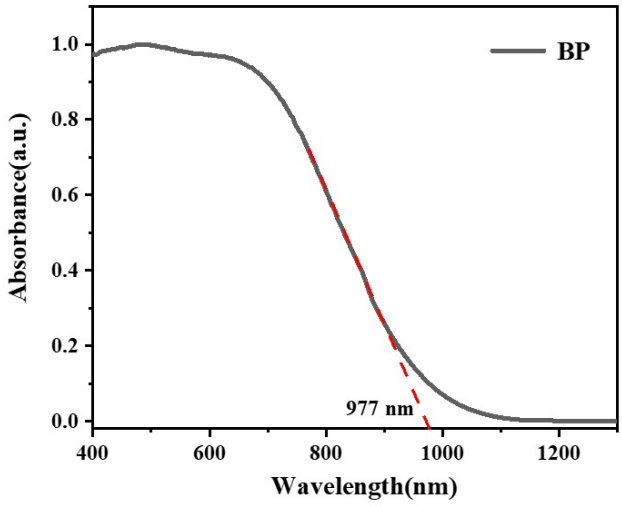

Figure S9. UV-vis absorption spectrum of BP.

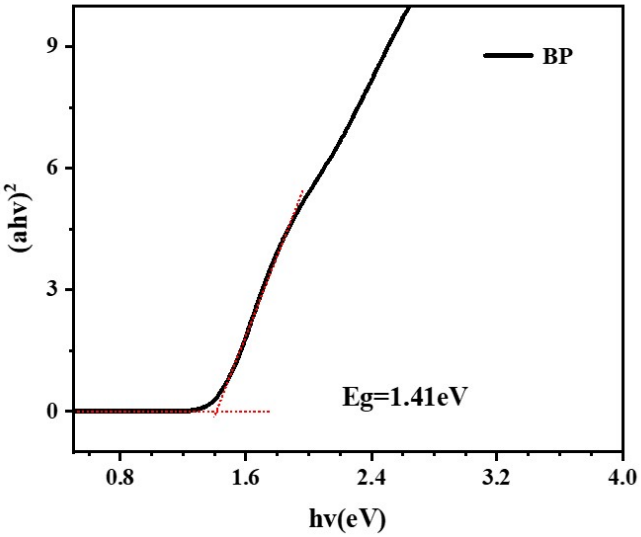

Figure S10. The band gap values of BP estimated from the plotted curves of $(\alpha h\nu)^2$ vs $h\nu$.

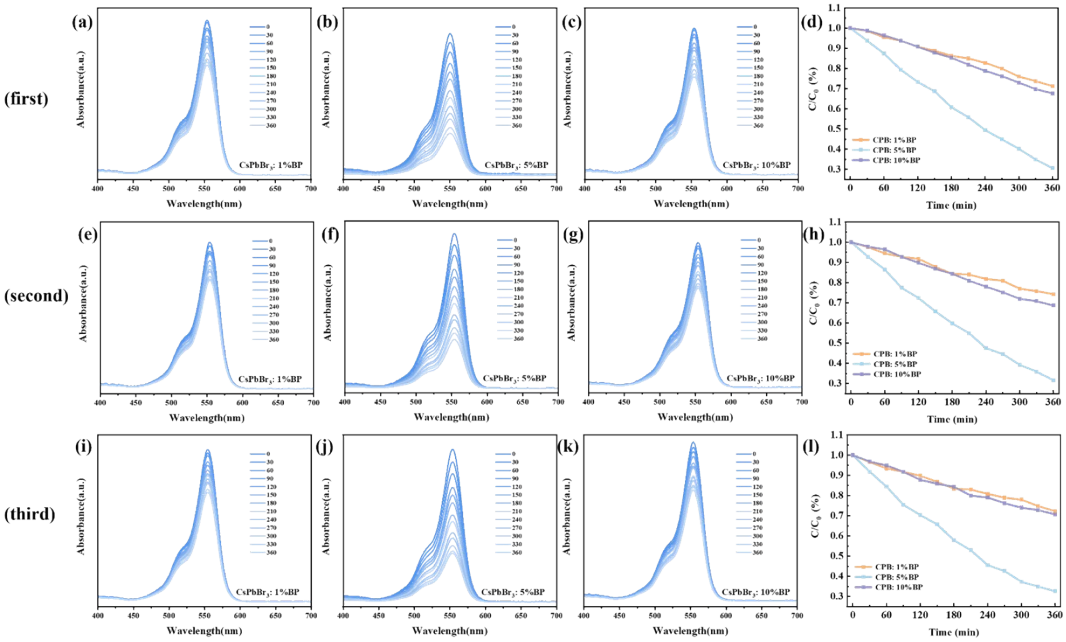

Figure S11. (a-c) Absorption spectra of the $CsPbBr_3$: x%BP (x% = 1%, 5%, 10%) systems for the first time under a 300 W xenon lamp for 6 hours, and (d) the first time C/C_0 plot vs irradiation time for $CsPbBr_3$: x%BP (x% = 1%, 5%, 10%). (e-g) Absorption spectra of the $CsPbBr_3$: x%BP (x% = 1%, 5%, 10%) systems for the second time under a 300 W xenon lamp for 6 hours, and (h) the second time C/C_0 plot vs irradiation time for $CsPbBr_3$: x%BP (x% = 1%, 5%, 10%). (i-k) Absorption spectra of the $CsPbBr_3$: x%BP (x% = 1%, 5%, 10%) systems for the third time under a 300 W xenon lamp for 6 hours, and (h) the third time C/C_0 plot vs irradiation time for $CsPbBr_3$: x%BP (x% = 1%, 5%, 10%).

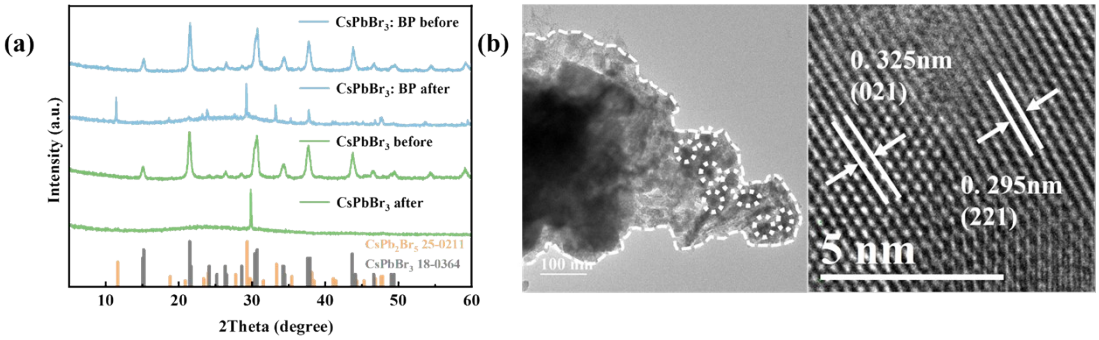

Figure S12. (a)XRD of $CsPbBr_3$ and $CsPbBr_3$: BP in aqueous solution of RhB with six hours under a 300 W Xe lamp. (b)TEM patterns of $CsPbBr_3$: BP in aqueous solution of RhB with six hours under a 300 W Xe lamp.

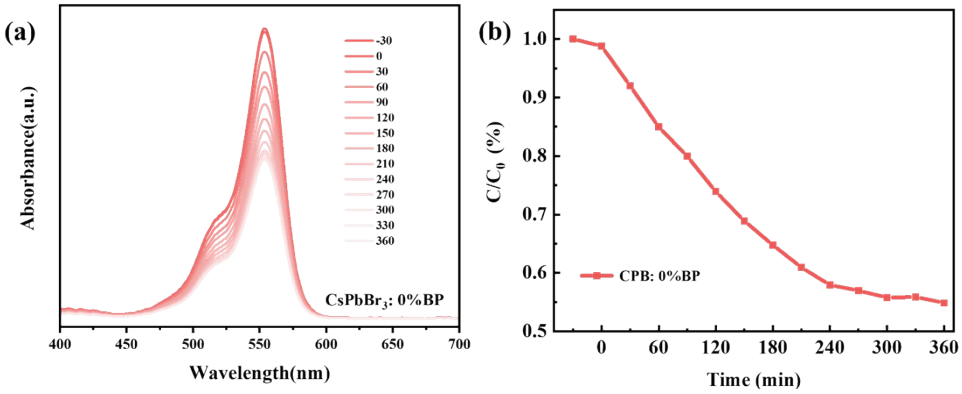

Figure S13. (a) Absorption spectra of the $CsPbBr_3$: 0%BP systems under a 300 W xenon lamp for 6 hours, and (b) C/C_0 plot vs irradiation time.

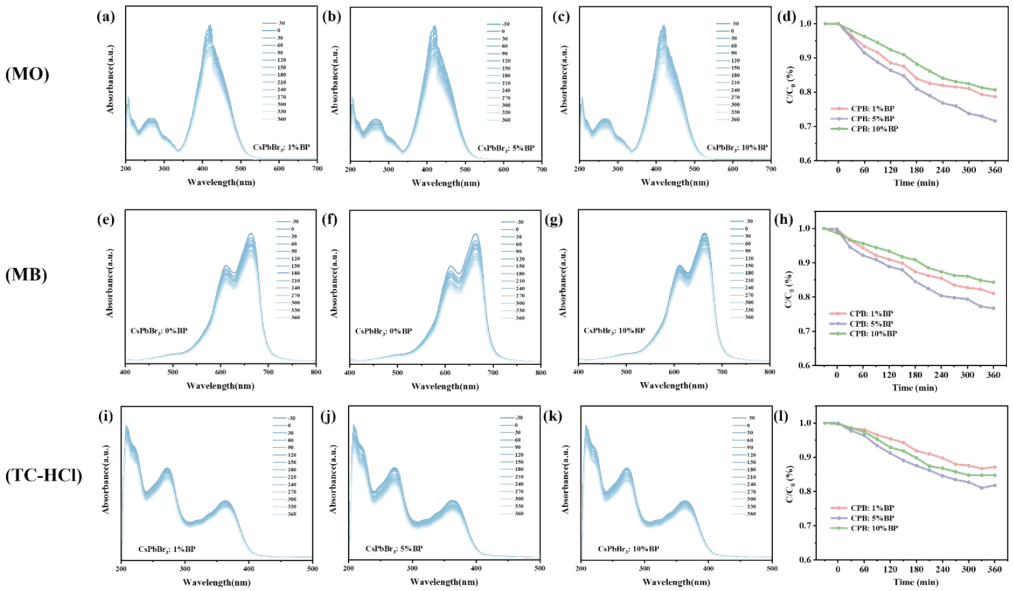

Figure S14. Absorption spectra and C/C_0 plots of MO (a-d), MB (e-h) and TC-HCl (i-l) degradation by $CsPbBr_3$: x%BP (x% = 1%, 5%, 10%) under a 300 W xenon lamp for 6 hours.

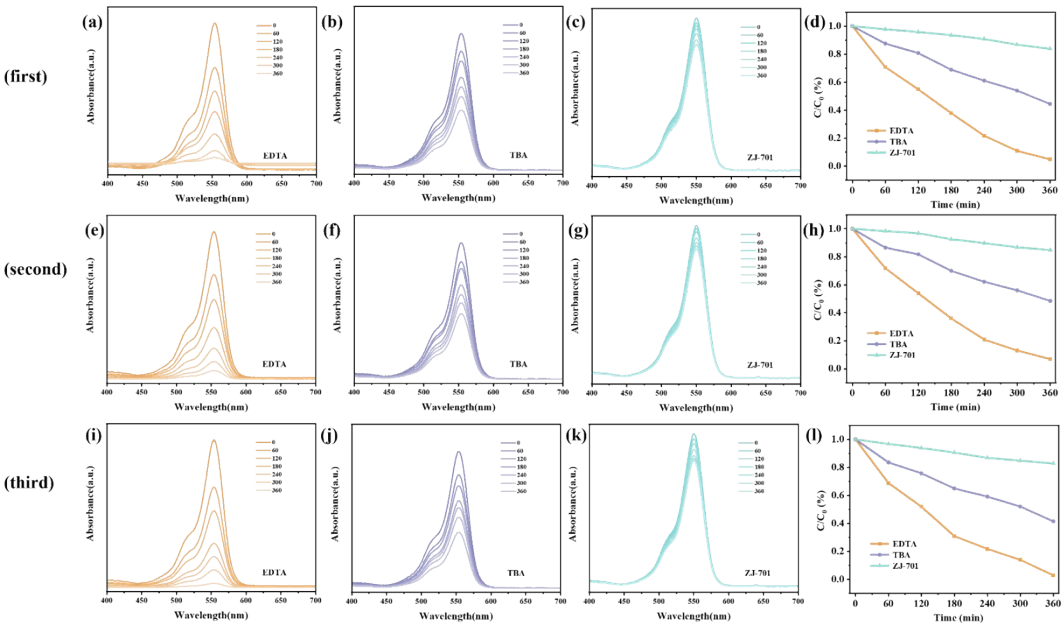

Figure S15. (a-c) The absorption spectra of the first EDTA, TBA and ZJ-701capture, and (d) the first photocatalytic degradation with scavengers. (e-g) The absorption spectra of the second EDTA, TBA and ZJ-701 capture, and (h) the second photocatalytic degradation with scavengers. (i-k) The absorption spectra of the third EDTA, TBA and ZJ-701capture, and (l) the third photocatalytic degradation with scavengers.

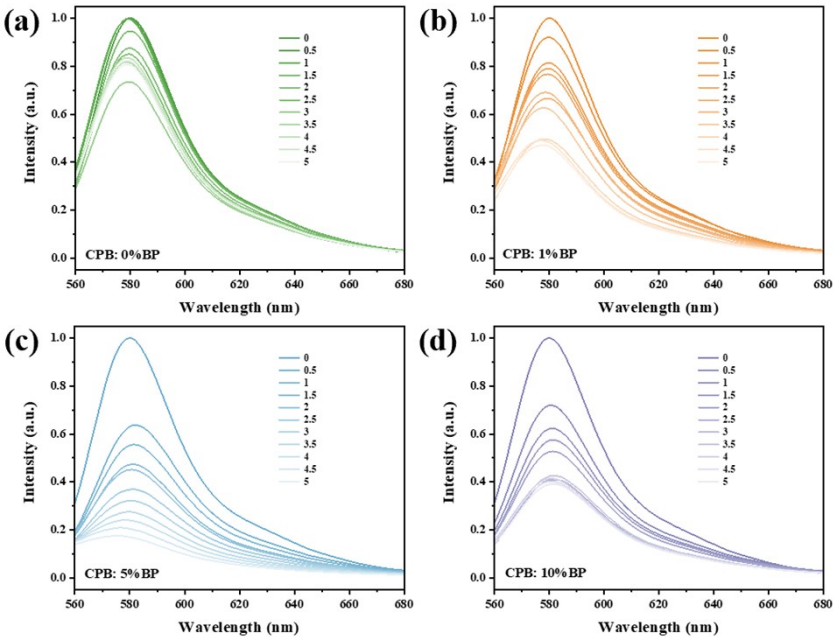

Figure S16. PL spectra of $CsPbBr_3$: x%BP (x%= 0%, 1%, 5%, 10%) systems with five hours under a 300 W Xe lamp.

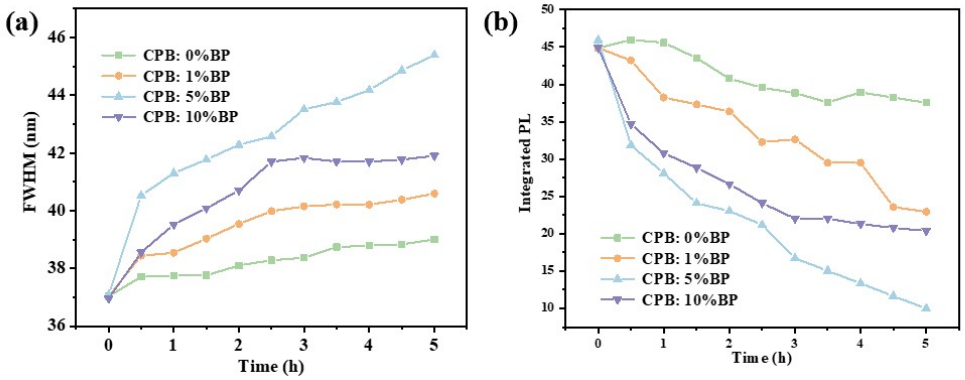

Figure S17. FWHM and Integrated PL spectra of $CsPbBr_3$: x%BP (x%= 0%, 1%, 5%, 10%) systems with five hours under a 300 W Xe lamp.

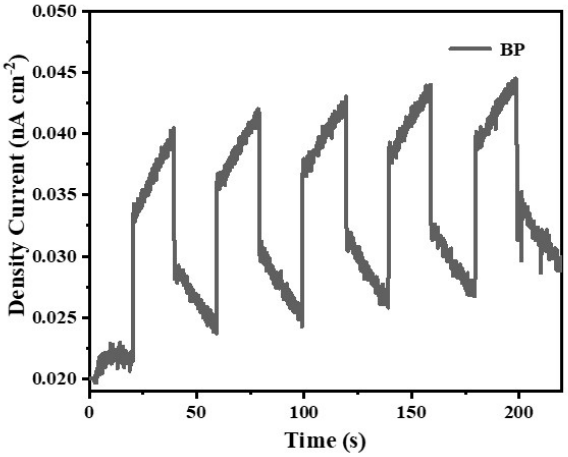

Figure S18. Transient photocurrent of pure BP.

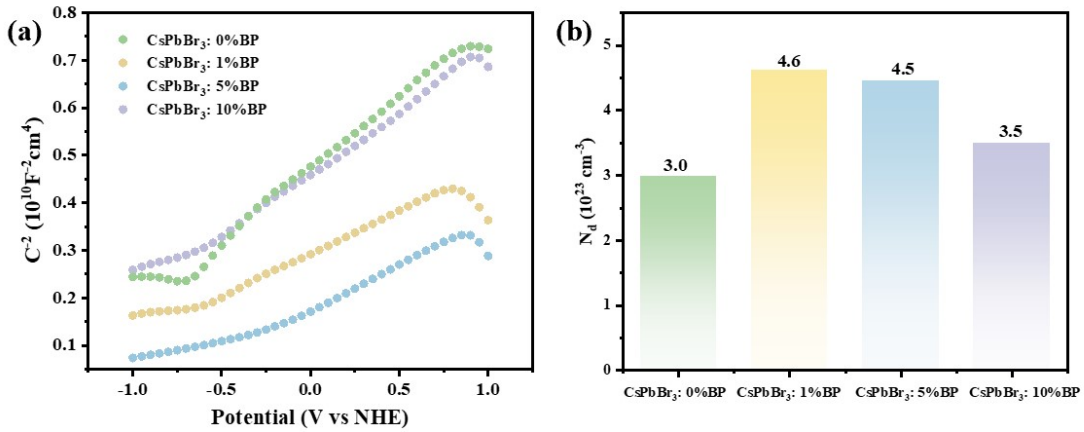

Figure S19. (a) Mott-Schottky curves and (b) the calculated N_d of $CsPbBr_3$: x%BP (x%= 0%, 1%, 5%, 10%).

S3. Tables

Table S1. The synthetic yields of $CsPbBr_3$: x%BP NCs (x% = 1%, 5%, 10%)

Sample	First (mg)	Second (mg)	Third (mg)	Fourth (mg)	Fifth (mg)	Average (mg)	Average （%）
BP	174.48	213.78	194.56	184.38	224.47	198.33±20.61	41.63±3.58
$CsPbBr_3$	112.45	121.46	113.46	102.36	108.36	111.62±7.02	48.13±3.03
$CsPbBr_3$: 1%BP	121.56	125.36	117.78	123.67	127.67	123.21±3.77	52.57±1.61
$CsPbBr_3$: 5%BP	156.36	148.78	152.37	147.38	151.36	151.25±3.48	62.11±1.43
$CsPbBr_3$: 10%BP	172.36	168.35	170.36	174.37	173.35	171.76±2.41	67.32±0.95

Table S2. Summary of the photocatalytic degradation performance of inorganic halide perovskites

Catalyst	Degraded substance	Degradation Efficiency	Literature
$CsPb_2Br_5$	RhB	50.45%	*Solid State Sciences 143 (2023) 107262*
$CsPbBr_3$	TC-HCl	6%	*Journal of Colloid and Interface Science 623 (2022) 974–984*
$CsPbBr_3$@SiO_2		75%	
$CsPbBr_3$: 5%BP	RhB	70%	*This article*